# Frequency Comb Generation Using a CMOS Compatible SiP DD-MZM for Flexible Networks

Jiachuan Lin, Hassan Sepehrian, Yelong Xu, Leslie A. Rusch, and Wei Shi

IEEE Photonics Technology Letters, (Volume 30, Issue 17) (2018)

Doi: 10.1109/LPT.2018.2856767

https://ieeexplore-ieee-org.acces.bibl.ulaval.ca/document/8412158/

# Frequency Comb Generation using a CMOS Compatible SiP DD-MZM for Flexible Networks

Jiachuan Lin, Hassan Sepehrian, *Student member, IEEE,* Yelong Xu, Leslie A. Rusch, *Fellow, IEEE, Fellow, OSA,* and Wei Shi, *Member, IEEE*

***Abstract*—On-chip frequency comb generation is a promising solution for seeding a chip-scale optical transmitter for both Nyquist wavelength-division multiplexing (WDM) and orthogonal frequency-division multiplexing. We demonstrate flexible frequency comb generation using a silicon photonic dual-drive Mach-Zehnder modulator fabricated on a CMOS-compatible process. Our on-chip comb has five lines spaced at 20 GHz, with a high tone-to-noise ratio of about 40 dB after one stage optical amplification. Our back-to-back transmission achieves bit error rates (BERs) well below 2e-2, the threshold for 20% overhead forward error correction (FEC), for 800 Gb/s using 16 Gbaud 32QAM on five WDM channels. We also test a seamless 800 Gb/s super-channel using 5×20 Gbaud 16QAM, with BER below the 7% overhead FEC threshold of 3.8e-3. To the best of our knowledge, this is the first demonstration of high-spectral-efficiency data carried by an all-silicon optical frequency comb. This establishes that a silicon optical frequency comb has sufficient optical signal to noise ratio for high order QAM, as well as excellent stability for super-channels without guard bands, paving the way to an integrated high-spectral-efficiency multi-carrier optical transmitter.**

***Index Terms*—optical frequency comb, silicon photonics, Nyquist-WDM, coherent detection**

## I. Introduction

Large-scale integration is an effective approach to lowering the cost and power consumption of a wavelength division multiplexing (WDM) transceiver [1]. Generation of multiple optical carriers is a very important part of a WDM transmitter, in terms of both overall chip complexity and power consumption. Either an integrated laser array or an optical frequency comb can achieve on-chip optical multi-carrier generation. An on-chip frequency comb provides a more compact and scalable solution than an integrated laser array. It also offers a locked frequency spacing that can be exploited for orthogonal frequency division multiplexing (OFDM) or super-channel Nyquist-WDM without guard bands, thus achieving high overall spectral efficiency (SE).

On-chip comb generation has been extensively studied on various semiconductor platforms, including silicon and InP. For generation of a large number of carriers, nonlinear processes [2][3] and mode locked lasers are typically employed. In [3], a silicon nitride micro-ring resonator was used to produce a notable high-quality frequency comb with 179 comb lines for 50 Tb/s transmission. A mode-locked laser having 107 flat comb lines was generated on an InP platform; an on-chip semiconductor optical amplifier was integrated as a gain media [4]. Despite these impressive demonstrations, it is challenging to manage a large number of comb lines in a real transmission system.

For an aggregate Tb/s data rate, especially in a modularly designed optical transceiver with a flexible grid, usually a few carriers are sufficient when using high-speed single-carrier data modulation [5, 6]. For long haul transmission, Tb/s using a single carrier is still very challenging and a simple and efficient on-chip, few-carrier generator is also preferred in this scenario. External-modulation-based combs, using phase modulation and/or amplitude modulation [7], offer several advantages, including a simple configuration, stable output, and tunable frequency spacing. In [8], an InP integrated phase modulator with an amplified feedback loop was reported for comb generation. In [9], an 11-line comb was generated using a tailored InP Mach-Zehnder modulator (MZM).

Compared to InP solutions, a silicon platform offers a smaller form factor and potentially lower unit cost. Using silicon-organic hybrid materials, a comb with 7-9 lines was generated by a silicon organic hybrid (SOH) MZM, and modulated with QPSK/16QAM to achieve Tb/s [10]. However, organic material is not CMOS-compatible and requires additional fabrication processes. An all-silicon solution is more attractive as it can leverage currently established silicon photonics factory processes. The all-silicon solution can be readily integrated with modulators, detector, and other passive components [11].

Combs with few lines were generated using all-silicon modulators in the following configurations: a single phase modulator (PM) [12], dual-parallel MZMs [13], a single micro-ring modulator (MRM) [14, 15] and cascaded MRMs [16]. Integration of an on-chip MRM comb generation and data modulation was recently demonstrated [16]. Compared to MZM solutions, a single PM based comb generation has less flexibility to achieve a flat output. The bandwidth advantage of dual-parallel MZMs over DD-MZM is outweighed by a more than double footprint (not only another MZM, but also increased distance between arms to isolate RF crosstalk) and

Manuscript received May 2018. This work was supported in part by Huawei Canada and NSERC (CRDPJ 486716-15). Authors are with ECE Department of Electrical and Computer Engineering., Centre for Optics, Photonics and Lasers (COPL), Université Laval, Quebec, G1V 0A6 Canada (e-mail: wei.shi@gel.ulaval.ca).

National Science and Engineering Research Council of Canada (NSERC) Funding: CRDPJ 486716-15

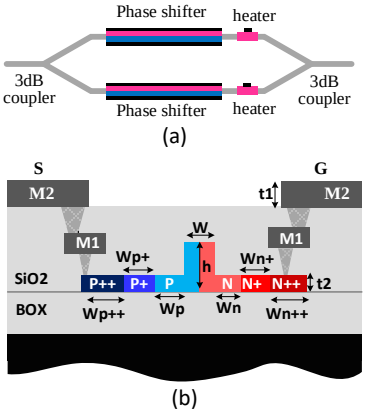


Fig1. (a) Illustration of the dual-drive MZM design, (b) cross section o MZM phase shifter: (all dimensions in μm) Wp++ = 5.2, Wp+ = 0.83, Wp = 0.37, Wn++ = 5.2, Wn+ = 0.81, Wn = 0.39, W = 0.5, h= 0.22, t1 = 2, t2 = 0.9

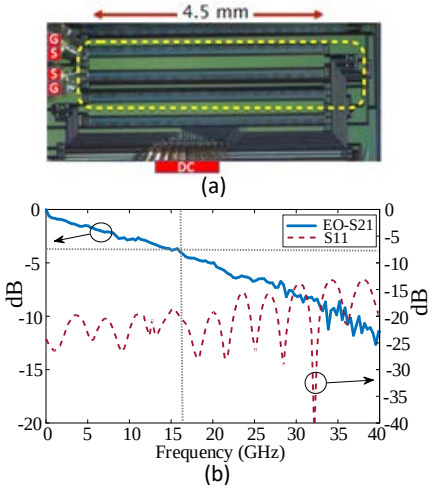


Fig. 2 (a) Photo of fabricated silicon modulator; (b) measured S11 and S21 of the silicon modulator when biased at -3.5V

implied increase in optical loss. All MRMs suffer from issues such as thermal sensitivity and self-heating, making it challenging to achieve high-power, stable comb lines.

In this letter, we experimentally generate a comb with five lines using a CMOS-compatible silicon dual-drive MZM (DD-MZM). Most demonstrations of silicon photonic modulators have adopted the single-drive push-pull configuration for high-speed data modulation. The dual-drive configuration enables a more compact design and flexible operation for flat frequency comb generation. In addition to flatness and optical signal to noise ratio, we further evaluate the quality of the comb as an on-chip comb-based Nyquist-WDM back-to-back system at aggregate bit rates up to 800 Gb/s. To the best of our knowledge, this is the first demonstration of high-spectral-efficiency data carried by an all-silicon optical frequency comb.

## II. Design and Fabrication of SiP DD-MZM

The structure of the DD-MZM, shown in Fig. 1a, consists of 3 dB couplers, a depletion-mode P-N junction for high-speed modulation, and a heater in each arm for fine-tuning the phase. We show the schematic of the silicon-diode phase shifter in cross-section in Fig. 1b, where physical dimensions are labeled. It is based on a rib waveguide in 220-nm silicon on insulator (SOI). The PN-junction is formed in the center of the waveguide. Doping densities of $5\times10^{17}$ cm$^{-3}$ and $3\times10^{17}$ cm$^{-3}$ are assumed in our design for p- and n-type respectively. The distance between heavy doping and waveguide boundary is set to 900 nm to trade-off radio frequency (RF) and optical loss. We designed a traveling-wave electrode using the model in [17]. The RF transmission line is terminated in 50 Ω, implemented on-chip using a doped resistor. The length of the phase shifter is 4.5 mm. The half-wave voltage of the designed MZM is around 6 V. The measured on-chip DD-MZM insertion loss is about 6.5 dB. The device was fabricated using a CMOS-compatible photonics foundry process at IME, Singapore, accessed via CMC Microsystems.

Figure 2a shows a photo of the fabricated silicon DD-MZM. The RF pads on the left, configured GS-SG are probed with the RF driving signals. We couple the diode bias voltage with the RF signals, and apply the combined drive signal through the same pads. The DC-voltage for heater control is applied through DC probes shown in the lower section of the photo.

We characterized the S parameters of the modulator using a 67 GHz vector network analyzer. Figure 2b shows the measured S21 and S11, indicating a modulator bandwidth of around 16.8 GHz for diodes reverse biased at -3.5 V. The S11 is below -10 dB for up to 40 GHz, indicating good 50 Ω matching. Surface grating couplers (GC) are used for optical I/O. The total optical coupling loss is around 16 dB (8 dB per coupler), as measured via a coupler-to-coupler device on the same chip.

## III. Experimental Setup

We generate a 5-line comb using the silicon DD-MZM fabricated per our design. To investigate the impact of optical signal to noise ratio (OSNR) and stability, the comb is modulated to carry Nyquist-WDM signals with different baud rates and modulation formats. The experimental test platform is shown in Fig. 3. The setup consists of two parts, as labeled in separate shaded areas of the setup: on-chip comb generation and Nyquist-WDM test.

In the on-chip comb generation section, a 16 dBm external cavity laser (ECL) with 100 kHz linewidth provides the seed carrier that is coupled to the silicon chip through a fiber array. The phase shifters of the MZM are driven by two sinusoidal RF signals generated by two synchronized Anritsu MG3691 signal synthesizers. The RF signals are amplified to 5 Vpp by two 18 dBm wide-band (50 GHz) RF drivers. The RF signals are coupled with a DC bias voltage via bias tees before applying them to the phase shifters. The DC voltage is used to operate the PN diode in reverse bias.

We adopt a dual-frequency driving scheme for 5-line generation, where the frequencies of the RF synthesizers are set to be 20 GHz (top arm) and 40 GHz (bottom arm). This dual-frequency driving scheme offers better OSNR and flatness than the single-frequency driving scheme as the RF driving swing is limited to a relative small voltage [18]. The combined RF and DC signals are then applied through a GS-SG configured RF probe. The MZM optical biasing is controlled by on-chip heaters on each MZM arm. At the output of the silicon chip, an erbium doped fiber amplifier (EDFA) is used to compensate for

National Science and Engineering Research Council of Canada (NSERC) Funding: CRDPJ 486716-15

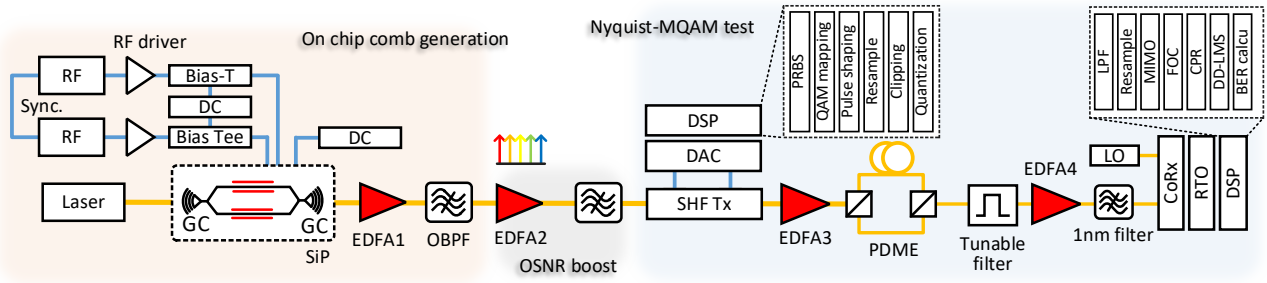


Fig. 3 Experimental setup for SiP on-chip comb generation and Nyquist-WDM back-to-back transmission.

coupling loss and on-chip loss. A tunable optical bandpass filter (OBPF) is placed after to suppress out-of-band amplified spontaneous emission (ASE) noise. We measure the comb signal spectrum using an APEX OSA with 100 MHz resolution.

Before the Nyquist-WDM test, the comb is boosted using another EDFA. Its spectrum is reshaped by a Waveshaper before QAM data modulation. The Waveshaper is programmed with a notched comb-like window for enhanced OSNR [19] and flatness. The total power of the 5-line comb is kept at 14 dBm. We test back-to-back transmission of 16/20 Gbaud 16QAM and 16 Gbaud 32QAM.

The transmitter digital signal processing (DSP) flow chart is shown in the insert of Fig. 3. A pseudo random bit sequence (PRBS) of order 19 is Gray coded to QAM symbols. The IQ symbols are then pulse shaped using a raised cosine finite impulse response (FIR) filter with a roll-off factor of 0.01. The pulse shaped samples are then resampled to match the DAC sampling rate, generating 16/20 Gbaud signal. These samples are clipped, quantized, and loaded to the 8-bit 64 GSa/s digital-to-analog converter (DAC). The data modulation is realized by driving a SHF optical QAM modulator with the Nyquist IQ signals. After data modulation, the Nyquist-WDM signal is amplified by EDFA3, followed by a polarization division multiplexing emulator (PDME), i.e., a pair of polarization beam splitter/combiners (PBS/C) and a delay line.

At the receiver end, the channel of interest is selected by a tunable optical filter. The selected channel is amplified by an EDFA and a 1 nm filter is used to reject out-of-band ASE noise. The signal is coherently detected using an integrated optical coherent receiver with 20 GHz electrical bandwidth, where the -3 dBm signal is mixed with the local oscillator (LO). The LO is implemented by a 14 dBm ECL laser, whose linewidth is ~5 kHz. The four outputs of the integrated coherent receiver (CoRx) are captured by a $4 \times 33$ GHz real time sampling oscilloscope (RTO) at a sampling rate of 80 GSa/s. The digitized samples are then processed using offline DSP.

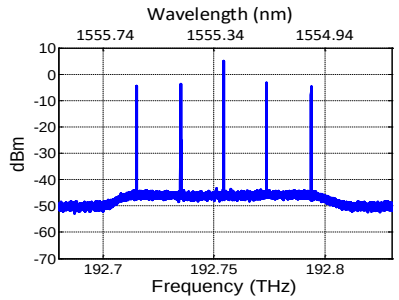


Fig. 4 Spectrum of generated 5-line comb with 20GHz spacing

The DSP stack is shown as an insert at receiver side in Fig. 3. We apply a $10^{th}$ order super Gaussian low pass filter (LPF) to all four captured signals and then resample to 2-samples per symbol. We use a real valued 4×4 multi-input-multi-output (MIMO) equalizer for polarization de-multiplexing and residual inter-symbol-interference (ISI) compensation. The frequency offset compensation (FOC) uses a FFT based method. The laser phase drifting is tracked using blind phase search with 32 test angles. After carrier phase recovery (CPR), a T-spaced 256-tap decision directed-least mean square (DD-LMS) filter is applied to further improve the signal quality. Finally, the recovered symbols are demodulated for BER calculation.

## IV. Results and Discussion

Figure 4 shows the spectrum of the 5-line comb with 20 GHz spacing that we generated, as measured after the OBPF. For comb generation, the diode reverse bias voltage of each silicon phase shifter is set to 0 V. This bias value trades-off modulation efficiency (bias-dependent $V_\pi$) and bandwidth. For a depletion-mode silicon phase shifter, the modulation efficiency varies with bias voltage due to the nonlinear plasma effect. With a smaller bias voltage, the silicon phase shifter exhibits better modulator efficiency leading to a lower $V_\pi$, but by sacrificing modulator bandwidth. For comb generation, the conversion efficiency is limited more by $V_\pi$ than by bandwidth. Across the five lines, the worst tone-to-noise ratio (TNR) measured (at 100 MHz resolution) is around 40 dB, corresponding to ~19 dB OSNR with a 0.1 nm noise reference bandwidth. However, the seed tone is much stronger and cannot be further suppressed. This is caused by the finite extinction ratio of ~14 dB of the SiP MZM, and should be improved through design optimization.

In the Nyquist-WDM test, as mentioned previously, the comb is further shaped using a programmable Waveshaper. This enables more consistent BER performance across all sub-channels. The Waveshaper is programmed as a comb filter with an additional 6 dB notch attenuation at the center frequency that improves the flatness and also boosts the OSNR. Figure 5a shows the reshaped comb lines. The Waveshaper was used for experimental convenience, but a comb filter and spectrum balancing filter could be realized in SiP [14, 20].

We set three benchmarks on the Nyquist-WDM system to evaluate the quality of the on-chip comb. We first modulate the 20 GHz spaced 5-line comb with $5 \times 16$ Gbaud Nyquist-16QAM. The modulated signal spectrum is shown in Fig. 5b, where we reserve a 4 GHz guard band between sub-channels. Then we expand the modulation constellation to further stress the OSNR of the comb, testing with a $5 \times 16$ Gbaud Nyquist-

National Science and Engineering Research Council of Canada (NSERC) Funding: CRDPJ 486716-15

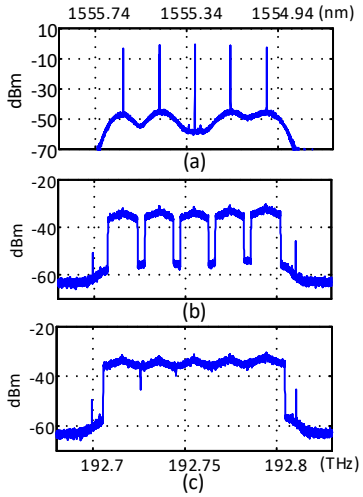


Fig. 5 Spectrums of (a) 20 GHz spaced 5-line comb after reshaping; (b) 5×16 Gbaud 16QAM; and (c) 5×20 Gbaud 16QAM

32QAM signal. In the final trial, we modulate the comb with a 5×20 Gbaud 16QAM signal, creating a super-channel without guard band. This extreme case demonstrates the good stability of the comb spacing, for which a seamless spectrum is shown in Fig 5c.

The BER test results are summarized in Fig. 6. We use pre-FEC BER thresholds to evaluate the system performance, assuming 3.8e-3 for 7% overhead hard decision FEC and 2e-2 for a 20% overhead soft decision FEC. As indicated by blue circles, the BERs for 16QAM at 5×16 Gbaud are well below 1e-3, achieving a net rate of 598 Gb/s for a 7% FEC overhead and a SE of 5.98 bit/s/Hz. For the 32QAM case, indicated by yellow diamonds, the BERs are all below the 20% FEC threshold, but the second and fourth channels show slightly higher BERs than the low overhead FEC threshold. The achieved net data rate is 667 Gb/s with SE of 6.67 bit/s/Hz. The BER of the super-channel (without guard band) is indicated by red squares in the same figure; the BERs are all below 3.8e-3. The results show negligible BER penalties from crosstalk induced by carrier frequency drift, demonstrating the stable frequency spacing between locked comb lines. With super-channel 16QAM, assuming a 7% (20%) FEC overhead we achieve a net rate of ~747 Gb/s (667 Gb/s) with SE of 7.47 bit/s/Hz (6.67 bit/s/Hz).

## V. Conclusion

Using an all-silicon DD-MZM, we experimentally achieved a 5-line frequency comb with 20 GHz spacing. The evaluation in the context of a Nyquist WDM system shows that the comb can well support 32QAM and no-guard-interval 16QAM. An 800 Gb/s super-channel (with a net rate of 747 Gb/s and an SE of 7.47 Gb/s/Hz) was demonstrated, indicating a promising solution for ultra-high-capacity optical transmitters using a CMOS-compatible process.

**Acknowledgement:** The authors thank Dr. Zhuhong Zhang and his team with Huawei Canada for many useful discussions. We also thank Nelson Landry for his technician support, and CMC Microsystems for the MPW service.

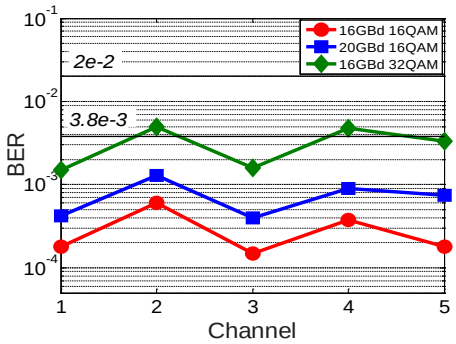


Fig. 6 BER results of Nyquist-WDM signals of 5×16Gbaud 16/32QAM and 5×20Gbaud 16QAM

## References

[1] V. Lal *et al*., "Extended C-band tunable multi-channel InP-based coherent transmitter PICs," *J. Lightwave. Technol.*, vol. 35, no. 7, pp. 1320-1327, Apr. 2017.
[2] J. Pfeifle *et al.*, "Coherent terabit communications with microresonator Kerr frequency combs," *Nat. Photonics*, vol. 8, no. 5, pp. 375-380, Apr. 2014.
[3] P. Marin-Palomo *et al.*, "Microresonator-based solitons for massively parallel coherent optical communications," *Nature*, vol. 546, no.7657, pp. 274-279, Jun. 2017.
[4] V. Corral *et al.*, "Optical frequency comb generator based on a monolithically integrated passive mode-locked ring laser with a Mach–Zehnder interferometer," *Opt. Lett*., vol. 41, no. 9, pp. 1937-1940, May 2016.
[5] R. Rios-Müller *et al.*, "1-Tb/s net data-rate transceiver based on single-carrier Nyquist-shaped 124 GBaud PDM-32QAM," in *Proc. OFC*, Los Angeles, CA, USA, 2015, pp. Th5B.1.
[6] D. S. Millar *et al*., "Design of a 1 Tb/s superchannel coherent receiver," *J. Lightwave. Technol*., vol. 34, no. 6, pp. 1453-1463, Mar. 2016.
[7] A. J. Metcalf, V. Torres-Company, D. E. Leaird and A. M. Weiner, "High-power broadly tunable electrooptic frequency comb generator," *IEEE J. Sel. Topics Quantum Electron*., vol 19, no. 6, pp. 231-236, Jul. 2013.
[8]N. Dupuis *et al.*, "InP-based comb generator for optical OFDM," *J. Lightwave. Technol*., vol. 30, no. 4, pp. 466-472, Feb. 2012.
[9] N. Yokota, K. Abe, S. Mieda and H. Yasaka, "Harmonic superposition for tailored optical frequency comb generation by a Mach–Zehnder modulator," *Opt. Lett.*, vol. 41, no. 5, pp. 1026-1029, Mar. 2016.
[10] C. Weimann *et al*, "Silicon-organic hybrid (SOH) frequency comb sources for Tb/s data transmission," *Opt. Express*, vol. 22, no. 3, pp. 3629-3637, Feb. 2014.
[11] P. Dong *et al.*, "Silicon in-phase/quadrature modulator with on-chip optical equalizer," *J. Lightwave. Technol.*, vol. 33, no. 6, pp. 1191-1196, Mar. 2015.
[12] K. P. Nagarjun *et al*., "Generation of tunable, high repetition rate optical frequency combs using on-chip silicon modulators," *Opt. Express*, vol. 26, no. 8, pp. 10744-10753, Apr. 2018.
[13] X. Xiao, M. Li, L. Wang, D. Chen, Q. Yang and S. Yu, "High speed silicon photonic modulators," in *Proc. OFC*, Los Angeles, CA, USA, 2017, pp. Tu2H.1.
[14] X. Wu and H. K. Tsang, "Flat-top frequency comb generation with silicon microring modulator and filter," in *Proc. CLEO*, San Jose, CA, USA, 2017, pp. SM4O.6.
[15] I. Demirtzioglou *et al.*, "Frequency comb generation in a silicon ring resonator modulator," *Opt. Express*, vol. 26, no. 2, pp. 790-796, Jan. 2018.
[16] Y. Xu *et al.*, "Integrated flexible-grid WDM transmitter using an optical frequency comb in microring modulators," *Opt. Lett.*, vol. 43, no. 7, pp. 1554-1557, Apr. 2018
[17] H. Bahrami, H. Sepehrian, C. S. Park, L. A. Rusch and W. Shi, "Time-domain large-signal modeling of traveling-wave modulators on SOI," *J. Lightwave. Technol*., vol. 34, no. 11, pp. 2812-2823, Jun. 2016.
[18] J. Lin, H. Sepehrian, L. A. Rusch and W. Shi, "Flexible on-chip frequency comb generation using a SOI dual-drive MZM," in *Proc. OI*, Santa Fe, NM, USA, 2017, pp. 27-28.
[19] J. Lin *et al.*, "Demonstration and evaluation of an optimized RFS comb for terabit flexible optical networks," *IEEE J. Opt. Commun. Netw*., vol. 9, no. 9: pp. 739-746, Sep. 2017.
[20] Z. Zou, L. Zhou, X. Li and J. Chen, "Channel-spacing tunable silicon comb filter using two linearly chirped Bragg gratings," *Opt. Express*, vol. 22, no. 16,

National Science and Engineering Research Council of Canada (NSERC) Funding: CRDPJ 486716-15